Plant Biotechnology 22(1), 39–45 (2005)

Original Paper

Physiological requirements of the nonmevalonate pathway for photo-acclimation in *Arabidopsis*

Masaya Hojo[1a], Masao Tasaka[1], Toshiharu Shikanai[1,2]*

[1] Graduate School of Biological Sciences, Nara Institute of Science and Technology, Ikoma, Nara 630-0192, Japan
[2] Graduate School of Agriculture, Kyushu University, Fukuoka 812-8581, Japan
*E-mail: shikanai@agr.kyushu-u.ac.jp Tel and Fax: +81-92-642-2882

Received December 8, 2004; accepted January 27, 2005 (Edited by T. Kohchi)

Abstract The nonmevalonate pathway produces isopentenyl diphosphate (IPP) in plastids, as does the mevalonate pathway present in the cytosol in higher plants. IPP is a precursor of an abundant array of isoprenoids, including pigments essential for photosynthesis. Two high-chlorophyll-fluorescence mutants, *isp1-1* and *isp1-2*, in which the *ispD* gene was partially inactivated, were characterzed. The *ispD* gene encodes 4-diphosphocytidyl-2-C-methyl-D-erythritol synthase, which functions in the third step of the nonmevalonate pathway in plastids. In mutant seedlings cultured at 50 μmol photons $m^{-2} s^{-1}$, the photosynthetic electron transport activity and chlorophyll content were reduced. The phenotype was partially suppressed in seedlings cultured at a relatively high light intensity of 300 μmol photons $m^{-2} s^{-1}$. These results suggest that the full activity of the nonmevalonate pathway is essential for photo-acclimation, particularly to low light conditions.

Key words: Nonmevalonate pathway, photo-acclimation

IPP is a precursor of an abundant array of isoprenoids involved in numerous roles in basic physiological processes including photosynthesis, respiration, development, reproduction and responses to environmental stress. In higher plants, IPP is synthesized by at least two different pathways (Figure 1), one of which takes palce in the cytosol (Newman and Chappell 1999) and the other in plastids (Lichtenthaler 1999; Rohmer 1999; Rodriguez-Concepcion and Boronat 2002). In the cytosol, three units of acetyl-CoA are condensed into 3-hydroxy-3-methylglutaryl-CoA (HMG-CoA), which is reduced to mevalonate. The subsequent phosphorylation and ATP-dependent decarboxylation produces IPP (mevalonate pathway). In plastids, however, IPP synthesis originates from glyceraldehyde 3-phosphate (G3P) and pyruvate, which are converted into 1-deoxy-D-xylulose 5-phosphate (DXP) by DXP synthase. The subsequent rearrangement and reduction of DXP leads to 2-C-methyl-D-erythritol 4-phosphate (MEP), which is converted into 4-diphosphocytidyl-2-C-methyl-D-erythritol (CDP-ME) via a reaction with CTP. The additional steps that ultimately lead to IPP (nonmevalonate pathway) were recently clarified in *Escherichia coli* (Rohdich et al. 2002; Kuzuyama 2002).

The *Arabidopsis thaliana* mutant *cla1*, in which the DXP synthase gene (*dxs*) is affected, displays impaired chloroplast development, leading to the albino phenotype in the seedling (Estevéz et al. 2000; Crowell et al. 2003). This result provides solid evidence that the nonmevalonate pathway functions to generate IPP in plastids. IPP is a precursor of carotenoids, the prenyl side-chains of chlorophylls and plastoquinones, which are indispensable in chloroplast development. Thus, at least during the early processes of chloroplast development, the mevalonate pathway cannot complement a defect in the nonmevalonate pathway.

The essential role of the nonmevalonate pathway in chloroplast development makes it difficult to apply a genetic approach in studying the physiological function of the nonmevalonate pathway. We have identified the weak alleles of the mutants partially defective in IPP synthesis in plastids as a good opportunity for this purpose. Since IPP is a source of a variety of isoprenoids, *isp1* mutations pleiotropically affect cellular function. This study focused on the function of the nonmevalonate pathway to assist in establishing the photosynthetic electron transport pathway in chloroplasts.

Abbreviations: CDP-ME, 4-diphosphocytidyl-2-C-methylerythritol; ETR, electron transport rate; IPP, isopentenyl diphosphate; MEP, 2-C-methyl-D-erythritol 4-phosphate; NPQ, nonphotochemical quenching.

[a] Present address: Nara Agricultural Experiment Station, 125 Sanguji, Haibara, Uda, Nara 633-0227, Japan

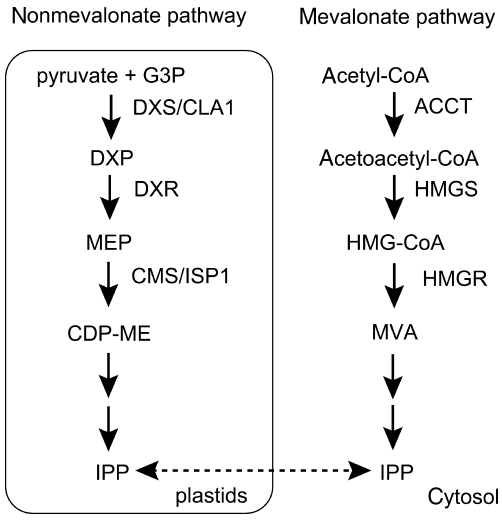

Figure 1. IPP synthesis pathways in the plant cell. G3P; glyceraldehyde 3-phosphate, DXP; 1-deoxy-D-xylulose 5-phosphate, MEP; 2-C-methyl-D-erythritol 4-phosphate, CDP-ME; 4-diphosphocytidyl-2-C-methyl- D-erythritol, HMG-CoA; 3-hydroxy-3-methylglutaryl-CoA, MVA; mevalonate; DXS; DX synthase, DXR; DX reductoisomerase, CMS; CDP-ME synthase, ACCT; acetoacetyl-CoA thiolase, HMGS; HMG-CoA synthase, HMGR; HMG-CoA reductase. *cla1* and *isp1* are enzyme names based on the *Arabidopsis* mutants.

Materials and methods

Plant materials and growth conditions

Plants were grown in Metromix potting soil under controlled conditions (light intensity of 50 μmol photons $m^{-2}\,s^{-1}$ or 300 μmol photons $m^{-2}\,s^{-1}$, 16-hr/8-hr light-dark cycle at 23°C). Both *isp1-1* and *isp1-2* were mutagenized using ethyl methanesulfonate (Shikanai et al. 1999).

Map-based cloning

The *isp1-1* mutation was mapped with cleaved amplified polymorphic sequence (CAPS) markers (Konieczny and Ausubel 1993). The oligonucleotide sequences and restriction enzymes of the markers used in the mapping are as follows: 5′-ACACTTCTAATGCCAAAGTGG-3′ and 5′-CTGTGCTCCATACTGATTACC-3′, *Rsa*I (COXI); 5′-TGCTTTCTGACTAATGCCAGG-3′ and 5′-AACCCT-AAGACTACGACTACG-3′, *Hae*III (T8K22.15). Genomic DNA was isolated from F_2 plants derived from a cross between *isp1-1* and the polymorphic wild type (Ladsberg *erecta*). Genomic *isp1* sequences containing the wild type and *isp* alleles were amplified by PCR using Ex-Taq DNA polymerase (Takara). The resulting PCR products were directly sequenced using a dye terminator cycle sequencing kit and an ABI prism377 sequencer (Perkin-Elmer).

For the complementation of the *isp1* mutations, the wild-type *isp1* sequence flanked by the sequences 5′-gaattcAACTCTCGGTTCAA-3′ and 5′- GCGAGCAC-AAATATggatcc-3′ was recovered from a BAC (bacterial artificial chromosome) clone, T8K22, and cloned in the plasmid pBI101. The lower case letters indicate restriction sites used in the cloning. The resulting plasmid was introduced into the *Agrobacterium tumefaciens* pMP90 strain and then transformed to *isp1-1* and *isp1-2*.

RT-PCR

Total cellular RNA was extracted from leaves using an RNeasy Plant Mini Kit (Qiagen) and was converted to cDNA using a SuperScrip™ Preamplification System (Boehringer). RT-PCR was carried out using the primers 5′-CAGTACATACCACTTCTTG-3′ and 5′-GGTTGG-AGCAGCTGTACTTG-3′. The products were cloned into the pGEM-T vector (Promega) and were then subjected to sequencing.

Chlorophyll fluorescence analysis

Chlorophyll fluorescence was measured with a MINI-PAM (pulse-amplitude modulation) fluorometer (Walz) as previously described (Schreiber et al. 1986). The minimum fluorescence of open photosystem II (PSII) centers (Fo) was excited by a weak measuring light (650 nm) at a light intensity of 0.05–0.1 μmol photons $m^{-2}\,s^{-1}$. A saturating pulse of white light (800 ms, 3,000 μmol photons $m^{-2}\,s^{-1}$) was applied to determine the maximum fluorescence of closed PSII centers in the dark-adapted state (Fm) and during actinic light illumination (Fm′). The steady-state fluorescence level (Fs) was recorded during actinic light illumination. NPQ (nonphotochemical quenching) was calculated as (Fm-Fm′)/Fm′. The quantum yield of PSII (Φ_{PSII}) was calculated as (Fm′–Fs)/Fm′ (Genty et al. 1989). The relative rate of electron transport through PSII (ETR) was calculated as $\Phi_{PSII}\times$light intensity (μmol photons $m^{-2}\,s^{-1}$).

Chlorophyll content determination

The chlorophyll content was determined by the absorbance changes in intact leaves using a SPAD-502 (Minolta). The data were standardized by the conventional method (Bruinsma 1961).

Results and discussion

isp1 *mutants are partially defective in the nonmevalonate pathway*

Two *isp1* mutants, *isp1-1* and *isp1-2*, were identified by their high-chlorophyll-fluorescence phenotypes at a light intensity of 300 μmol photons $m^{-2}\,s^{-1}$ (Figure 2). Since the seedlings used in the screening were cultured at 50 μmol photons $m^{-2}\,s^{-1}$, the light intensity of 300 μmol photons $m^{-2}\,s^{-1}$ was relatively high. The genetic analysis established that both *isp1* mutations are recessive, with both mutations on a single gene (data not shown). *isp1-1*

and *isp1-2* were previously referred to as CE12-10 and CE11-4, respectively (Shikanai et al. 1999), and named after the *ispD* gene responsible for the phenotype (see below). In addition to the high-chlorophyll-fluorescence phenotype, the growth rate in the soil was reduced at 50 μmol photons $m^{-2} s^{-1}$ in both alleles (Figures 2, 6). The chlorophyll content was also reduced to 70% and 30% of that in the wild type in *isp1-1* and *isp1-2*, respectively, when seedlings were cultured at 50 μmol photons $m^{-2} s^{-1}$ (Table 1). The phenotype of *isp1-2* was severer than that in *isp1-1*.

The gene affected in *isp1* was identified by map-based cloning (Figure 3). The *isp1-1* (Col *gl1* background) was crossed with the polymorphic wild type (Landsberd *erecta*). The mutation was mapped on the north region of chromosome 2. Fine mapping using 266 F_2 plants identified an approximately 50-kb region flanked by two molecular markers, COXI and T8K22.15 on BAC clones T16F16 and T8K22, respectively. Since *isp1* mutants were identified by their high-chlorophyll-fluorescence phenotype, it was probable that the defects were closely related to chloroplast function. Therefore, the genomic sequences of candidate genes encoding predicted chloroplast-targeting proteins were determined. Finally, sequence alterations were found in both alleles in *ispD* (At2g02500) encoding CDP-ME synthase (Rohdich et al. 2000).

To confirm that the *isp1* phenotypes were due to mutations in *ispD*, a wild-type sequence of At2g02500 was introduced into both *isp1-1* and *isp1-2*. The transformation fully complemented the phenotypes both in the chlorophyll fluorescence level and the growth rate that could be evaluated by seedling size (Figure 2, *isp1-1+isp1* and *isp1-2+isp1*). We conclude that the *isp1* phenotypes were due to lesions in *ispD*.

In *isp1-1*, arginine was substituted for glycine[154]. The glycine residue is highly conserved among enzymes from bacteria to higher plants (Figure 4A). In contrast, a severe allele, *isp1-2*, has a nucleotide substitution at a splicing junction between the fifth intron and the sixth exon, from the conserved AG to AA (Figure 4B). To confirm the possible *isp1-2* defect due to the miss-splicing, a cDNA sequence containing the fifth and sixth exons was amplified by RT-PCR and cloned. Sequence determination of the clones confirmed that the fifth intron was spliced out using a cryptic splicing consensus AG that was nine nucleotides down-stream of the authentic splicing consensus, resulting in the splicing out of the first nine nucleotides of the sixth exon from the mature RNA (Figure 4B). Consequently, *isp1-2* lacks three amino acids, glutamate[139]-tyrosine[140]-glutamate[141]. Although these three amino acids are not conserved in the bacterial enzymes (Figure 4A), this deletion must severely impair the activity of the enzyme considering the severer phenotype of *isp1-2* compared with that of *isp1-1*.

ISP1/CMS catalyzes the conversion of MEP into CDP-ME via a reaction with CTP (Figure 1). The reaction is the third step in IPP synthesis in the nonmevalonate pathway. The nonmevalonate pathway is essential in chloroplast development, as was suggested by an albino phenotype of *cla1* (Mandel et al. 1996). Since *ISP1* is a single copy gene encoding a unique route

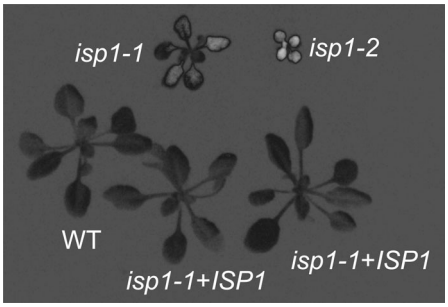

Figure 2. Chlorophyll fluorescence imaging. The wild-type and *isp1* seedlings were grown in soil for four weeks. A chlorophyll fluorescence image was captured after a 1-min illumination with actinic light (300 μmol photons $m^{-2} s^{-1}$). WT; Columbia *gl1*, *isp1-1+ISP1*, *isp1-2+ISP1*; *isp1* mutants transformed with the genomic *isp1* sequence. Brighter images mean higher levels of chlorophyll fluorescence.

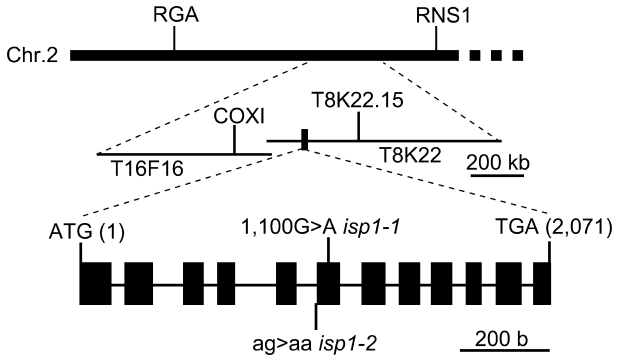

Figure 3. Map-based cloning of *isp1*. *isp1* was mapped to the 50-kb region flanked by two molecular markers, COXI and T8K22.15 on BAC clones T16F16 and T8K22, respectively. The small box on T8K22 represents the position of *ISP1*. Exons and introns were previously predicted from the cDNA sequence (Rohdich et al. 2000). Vertical bars on the gene indicate the positions of the *isp1* mutations.

Table 1. Chlorophyll content in the seedlings cultured at each light intensity.

	Wild type	*isp1-1*	*isp1-2*
50 mmol photons $m^{-2} s^{-1}$	18.2±1.0	12.6±0.8	5.5±1.5
300 μmol photons $m^{-2} s^{-1}$	21.6±1.4 (119%)	17.3±2.3 (137%)	7.0+/−3.0 (127%)

Wild type and *isp1* seedlings were cultured for three weeks and chlorophyll content ($\mu g/cm^2$ leaf area) was determined. Values are means±standard deviations (n=5). The rate of increase is indicated in parentheses.

of the pathway, the complete loss of the enzyme activity must lead to an albino phenotype. This idea was supported by the fact that severe repression of *isp1* expression by antisense RNA caused an albino phenotype (Okada et al. 2002). Consistent with the mild phenotype in both *isp1* alleles, the *isp1* defects were due to an amino acid alteration in *isp1-1* and a deletion of three amino acids in *isp1-2*. We conclude that both of the alleles of *isp1* are partially defective in their CDP-ME synthase activity.

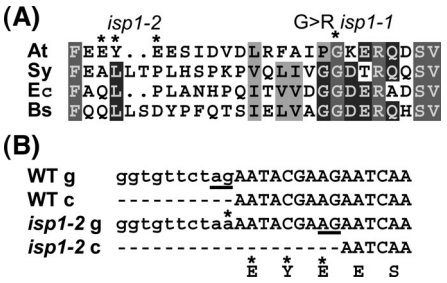

Figure 4. The *isp1* mutation points. (A) Alignment of a part of 4-diphosphocytidyl-2C-methyl-d-erythritol synthase sequences containing *isp1* mutations. An arginine substituted for glycine in *isp1*-1 and a three amino acid deletion in *isp1*-2 are indicated by asterisks. At, *Arabidopsis thaliana isp1*; Sy, *Synechocystis* species strain PCC6803; Ec, *Escherichia coli*; Bs, *Bacillus subtilis*. (B) Alignment of the junction of the fifth intron and the sixth exon from genomic (g) and cDNA (c) sequences of the wild type (WT, columbia) and *isp1-2*. A mutation point and the resulting three amino acid deletions are indicated by asterisks. Consensus AG sequences for the splicing are underlined.

Characterization of the isp1 *defect in photosynthetic electron transport*

isp1 mutants were identified based on their high-chlorophyll-fluorescence phenotype, indicating that the defect is related to photosynthetic electron transport. To characterize the *isp1* defect further, both alleles were analyzed by PAM chlorophyll fluorometry. Figure 5A shows the light intensity dependence of a chlorophyll fluorescence parameter of the electron transport rate (ETR). The ETR represents the relative amount of electrons passing through PSII during steady-state photosynthesis (see materials and methods). In *isp1* mutants, the ETR was drastically reduced over the entire light intensity range. The ETR was saturated at a lower light intensity (approximately 100 μmol photons $m^{-2}\,s^{-1}$) at a lower level in *isp1-1* (30% of the maximum ETR in the wild type) and at the same light intensity at a much lower level (less than 20% of the maximum ETR

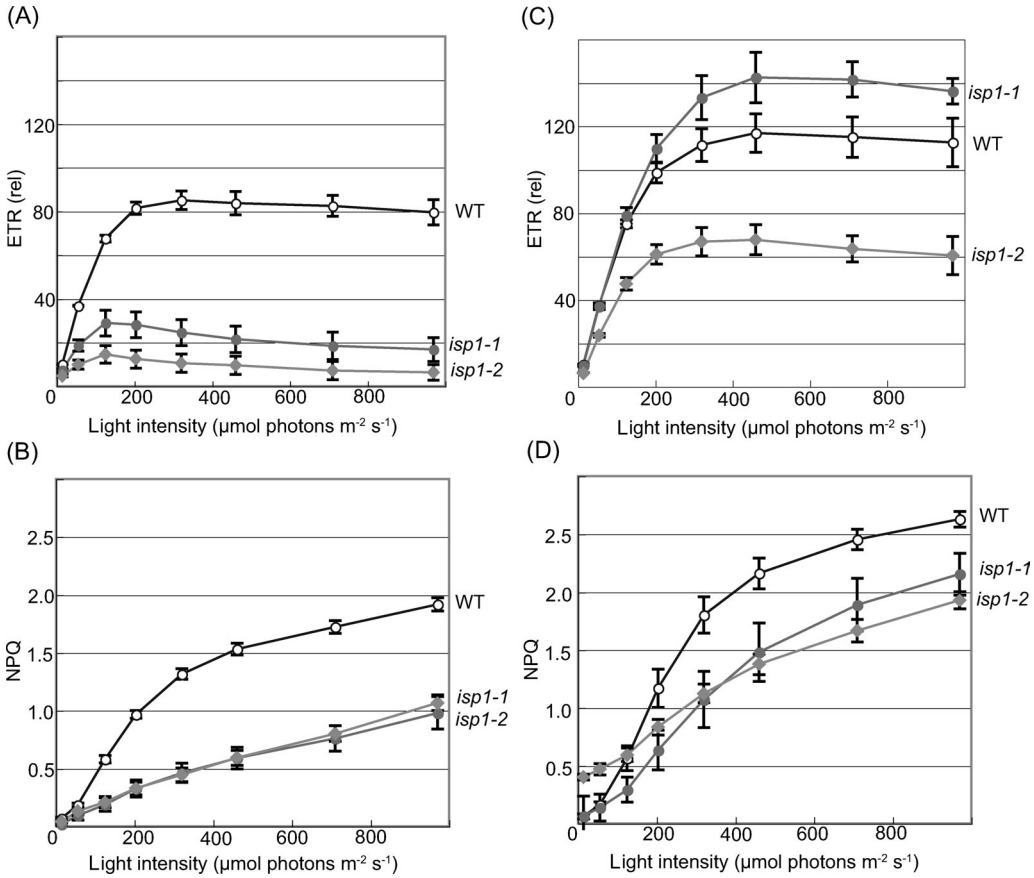

Figure 5. Light intensity dependence of the chlorophyll fluorescence parameters. (A, C) Light intensity dependence of ETR (relative value). (B, D) Light intensity dependence of NPQ. Seedlings were cultured at 50 μmol photons $m^{-2}\,s^{-1}$ in (A) and (B) and at 300 μmol photons $m^{-2}\,s^{-1}$ in (C) and (D) for three weeks. Each point represents the mean±standard deviation (n=5).

Table 2. Maximum activity of PSII (Fm/Fm) in the seedlings cultured at each light intensity.

	Wild type	*isp1-1*	*isp1-2*
50 μmol photons $m^{-2} s^{-1}$	0.80±0.00	0.75±0.08	0.68±0.02
300 μmol photons $m^{-2} s^{-1}$	0.82±0.01	0.82±0.00	0.71±0.01

Wild type and *isp1* seedlings were cultured for three weeks and Fv/Fm was measured by PAM chlorophyll fluorometry. Values are means±standard deviations (n=5).

in the wild type) in *isp1-2*.

Figure 5B shows the light intensity dependence of another chlorophyll fluorescence parameter, NPQ (see Materials and methods). In higher plants, a major factor in NPQ is thermal dissipation, in which absorbed excessive light energy is dissipated safely as heat from PSII antennae (Muller et al. 2001). The induction of thermal dissipation is triggered by the acidification of the thylakoid lumen (less than pH6.0), which occurs under excessive light conditions (Munekage et al. 2001). The reduced ETR led to an insufficient ΔpH across the thylakoid membranes, and consequently, to a reduced NPQ activity in both alleles of *isp1* (Figure 5B). Thus, the high-chlorophyll-fluorescence phenotype of *isp1* can be characterized by the reduction in both photochemical quenching and NPQ of chlorophyll fluorescence.

Another characteristic of *isp1* mutants is a reduction in a chlorophyll fluorescence parameter, Fv/Fm (see Materials and methods) representing the maximum activity of PSII photochemistry (Table 2). The reduction in Fv/Fm is potentially due to the impaired PSII photochemistry by photo-inhibition (Krause and Weis, 1991). Since *isp1* mutants responded better to higher light intensity for growth (see below), it is unlikely that *isp1* seedlings were photo-damaged even at the low light intensity of the culture conditions (50 μmol photons $m^{-2} s^{-1}$). A reduction in Fv/Fm was also observed when the proper assembly of functional PSII is arrested such as by a defect in a PSII subunit gene (Murakami et al. 2002) or impaired protein synthesis in chloroplasts (Kishine et al. 2004). Since the nonmevalonate pathway is involved in the synthesis of pigments in PSII, chlorophyll and plastoquinone, it is probable that PSII assembly was partially impaired in *isp1* due to the limited availability of these pigments.

Partial suppression of the isp1 *phenotype by high light intensity*

It was observed that *isp1* mutants grew better in a greenhouse, where the maximum light intensity was up to 1,000 μmol photons $m^{-2} s^{-1}$, than in a growth chamber at 50 μmol photons $m^{-2} s^{-1}$. To analyze the effect of different light intensities on the *isp1* phenotype in detail, we compared seedlings cultured at 50 μmol photons $m^{-2} s^{-1}$ and 300 μmol photons $m^{-2} s^{-1}$. A light intensity of 300 μmol photons $m^{-2} sec^{-1}$ is not stressful for *Arabidopsis* seedlings, in so far as the light intensity is constant and the other culture conditions, watering,

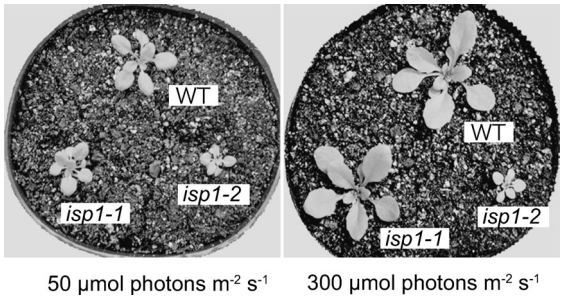

Figure 6. The wild-type (WT), *isp1-1* and *isp1-2* seedlings cultured at light intensities of 50 μmol photons $m^{-2} s^{-1}$ and 300 μmol photons $m^{-2} s^{-1}$ for three weeks.

humidity and temperature, are optimized. In contrast, it is known that the mesophyll cells of a leaf do not elongate in seedlings cultured at 50 μmol photons $m^{-2} s^{-1}$ (Pyke and López-Juez 1999), suggesting that this light intensity is too low for *Arabidopsis*. Thus, the range of light intensity used in this assay was from a low light intensity (50 μmol photons $m^{-2} s^{-1}$) to a more desirable intensity for plants (300 μmol photons $m^{-2} s^{-1}$).

The *isp1-1* seedlings cultured at 300 μmol photons $m^{-2} s^{-1}$ were almost indistinguishable from the wild-type seedlings cultured at the same light intensity, while the *isp1-2* seedlings still exhibited the strong phenotype (Figure 6). As shown in Table 1, an increase in the growth light intensity from 50 μmol photons $m^{-2} s^{-1}$ to 300 μmol photons $m^{-2} s^{-1}$ increased the chlorophyll content par unit of leaf area (119% in the wild type). A similar response to an increase in light intensity was observed in both *isp1-1* (137%) and in *isp1-2* (127%), although the chlorophyll content did not recover to the wild-type level.

The phenotype in Fv/Fm was also evaluated in seedlings grown at 300 μmol photons $m^{-2} s^{-1}$ (Table 2). Consistent with the restoration of the growth rate in *isp1-1*, Fv/Fm completely recovered to the wild-type level, suggesting that PSII is fully functional in *isp1-1*. In contrast, Fv/Fm was still significantly affected in *isp1-2*.

Figure 5 (C, D) shows the light intensity dependence of the chlorophyll fluorescence parameters, ETR and NPQ, which can be compared with those of seedlings cultured at 50 μmol photons $m^{-2} s^{-1}$ (Figure 5A, B). In the wild type, a shift in the growth light intensity from 50 μmol photons $m^{-2} s^{-1}$ to 300 μmol photons $m^{-2} s^{-1}$ increased the maximum ETR level (135%). This change is partly due to differences in the leaf development stage

between seedlings cultured under the two light conditions, since a similar level of ETR was achieved in the fully expanded leaves of seedlings cultured for a longer period (4 weeks), even when cultured at 50 μmol photons $m^{-2} s^{-1}$. It is also probable that the increase in ETR was partly due to the photo-acclimation to a relatively high light intensity, since the leaf structure is apparently different between seedlings cultured at different light intensities (Pyke and López-Juez 1999). Unexpectedly, ETR of *isp1-1* cultured at 300 μmol photons $m^{-2} s^{-1}$ was higher than that in the wild type. However, since the chlorophyll content was still lower in *isp1-1* than in the wild type, even when cultured at 300 μmol photons $m^{-2} s^{-1}$, the net amount of electrons passing through PSII (net ETR) and the resulting CO_2 fixation may not have been significantly higher in *isp1-1* than in the wild type. To estimate the net ETR, a relative ETR should be compensated by the light absorptance by leaves (a factor representing how efficiently light energy is absorbed by PSII antennae), which is correlated with the chlorophyll content. Taken together with the recovery of Fv/Fm (Table 2), the recovery of the ETR fully explains the wild-type-like growth rate of *isp1-1* at 300 μmol photons $m^{-2} s^{-1}$. Recovery of the ETR was also observed in *isp1-2* cultured at 300 μmol photons $m^{-2} s^{-1}$, although the level was still significantly lower than in the wild type.

Although the ETR was almost completely restored in *isp1-1*, NPQ induction was not fully restored (Figure 5B, D). The results indicate that the *isp1-1* defect was not completely suppressed, especially regarding the photo-acclimation capacity to different light intensities. In *isp1-2*, NPQ induction also did not recover when cultured at 300 μmol photons $m^{-2} s^{-1}$.

The *isp1-1* defect was rather alleviated especially in terms of the ETR and the growth rate when the seedlings were cultured at 300 μmol photons $m^{-2} s^{-1}$ (Figures 5, 6). This light intensity is more desirable for plants than the lower light intensity of 50 μmol photons $m^{-2} s^{-1}$, and the mutant seedlings may have optimized the photosynthetic machinery for maximum growth, even though the nonmevalonate pathway was not fully active. However, the phenotype was not completely suppressed in terms of NPQ (Figure 5C, D) and chlorophyll content (Table 2), suggesting that the higher activity of the nonmevalonate pathway is required for full acclimation. The *isp1-1* seedlings may be sensitive to the natural environmental conditions, in which the light intensity is high enough but tends to fluctuate, due to the incomplete acclimation to high light intensity. However, a much more drastic phenotype was observed when the *isp1-1* seedlings were cultured at a lower light intensity (50 μmol photons $m^{-2} s^{-1}$). This result indicates that the full activity of the nonmevalonate pathway is essential for plants to adapt to low light conditions.

Acknowledgements

We thank Momoko Miyata for her excellent technical assistance. We also thank Prof. Yuji Kamiya (RIKEN) and Prof. Kazufumi Yazaki (Kyoto University) for their helpful discussions. This work was supported by grants from JSPS.

References

Bruinsma J (1961) A comment on the spectrophotometric determination of chlorophyll. *Biochim Biophys Acta* 52: 576–578

Crowell DN, Packard CE, Pierson CA, Giner JL, Downes BP, Chary SN (2003) Identification of an allele of *CLA1* associated with variegation in *Arabidopsis thaliana*. *Physiol Plant* 118: 29–37

Estevéz JM, Cantero A, Romero C, Kawaide H, Jiménez LF, Kuzuyama T, Seto H, Kamiya Y, Leon P (2000) Analysis of the expression of *cla1*, a gene that encodes the 1-deoxyxylulose 5-phosphate synthase of the 2-C-methyl-D-erythritol-4-phosphate pathway in *Arabidopsis.* *Plant Physiol* 124: 95–104

Genty B, Briantais J-M, Baker NR (1989) The relationship between quantum yield of photosynthetic electron transport and quenching of chlorophyll fluorescence. *Biochim Biophys Acta* 990: 87–92

Kishine M, Takabayashi A, Munekage Y, Shikanai T, Endo T, Sato F (2004) Ribosomal RNA processing and an RNase R family member in chloroplasts of *Arabidopsis*. *Plant Mol Biol* 55: 595–606

Konieczny A, Ausubel FM (1993) A procedure for mapping *Arabidopsis* mutations using co-dominant ecotype-specific PCR-based markers. *Plant J* 4: 403–410

Krause GH, Weis E (1991) Chlorophyll fluorescence and photosynthesis: The basics. *Annu Rev Plant Physiol Plant Mol Biol* 42: 313–349

Kuzuyama T (2002) Mevalonate and nonmevalonate pathways for the biosynthesis of isoprene units. *Biosci Biotechnol Biochem* 66: 1619–1627

Lichtenthaler HK (1999) The 1-deoxy-D-xylulose-5-phosphate pathway of isoprenoid biosynthesis in plants. *Annu Rev Plant Physiol Plant Mol Biol* 50: 47–65

Mandel MA, Feldmann KA, Herrera-Estrella L, Rocha-Sosa M, León P (1996) *cla1*, a novel gene required for chloroplast development, is highly conserved in evolution. *Plant J* 9: 648–658

Muller P, Li XP, Niyogi KK (2001) Non-photochemical quenching. A response to excess light energy. *Plant Physiol* 125: 1158–1166

Munekage Y, Takeda S, Endo T, Jahns P, Hashimoto T, Shikanai T (2001) Cytochrome b_6f mutation specifically affects thermal dissipation of absorbed light energy in *Arabidopsis*. *Plant J* 28: 351–359

Murakami R, Ifuku K, Takabayashi A, Shikanai T, Endo T, Sato F (2002) Characterization of an *Arabidopsis thaliana* mutant with impaired *psb*O, one of two genes encoding extrinsic 33-kDa proteins in photosystem II. *FEBS lett* 523: 138–142

Newman JD, Chappell J (1997) Isoprenoid biosynthesis in plants: carbon partitioning within the cytoplasmic pathway. *Crit Rev Biochem Mol Biol* 34: 95–106

Okada K, Kawaide H, Kuzuyama T, Seto H, Curtis IS, Kamiya Y (2002) Antisense and chemical suppression of the nonmevalonate pathway affects ent-kaurene biosynthesis in

Arabidopsis. *Planta* 215: 339–344

Pyke K, López-Juez E (1999) Cellular differentiation and leaf morphogenesis in *Arabidopsis*. *Crit Rev Plant Sci* 18: 527–546

Rodriguez-Concepcion M, Boronat A (2002) Elucidation of the methylerythritol phosphate pathway for isoprenoid biosynthesis in bacteria and plastids. A metabolic milestone achieved through genomics. *Plant Physiol* 130: 1079–1089

Rohdich F, Wungsintaweekul J, Eisenreich W, Richter G, Schuhr CA, Hecht S, Zenk MH, Bacher A (2000) Biosynthesis of terpenoids: 4-diphosphocytidyl-2C-methyl-D-erythritol synthase of *Arabidopsis thaliana*. *Proc Natl Acad Sci USA* 97: 6451–6456

Rohdich F, Hecht S, Gartner K, Adam P, Krieger C, Amslinger S, Arigoni D, Bacher A, Eisenreich W (2002) Studies on the nonmevalonate terpene biosynthetic pathway: metabolic role of IspH (LytB) protein. *Proc Natl Acad Sci USA* 99: 1158–1163

Rohmer M (1999) The discovery of a mevalonate-independent pathway for isoprenoid biosynthesis in bacteria, algae and higher plants. *Nat Prod Rep* 16: 565–574

Schreiber U, Schliwa U, Bilger W (1986) Continuous recording of photochemical and non-photochemical chlorophyll fluorescence quenching with a new type of modulation fluorometer. *Photosynth Res* 10: 51–62

Shikanai T, Munekage Y, Shimizu K, Endo T, Hashimoto T (1999) Identification and characterization of *Arabidopsis* mutants with reduced quenching of chlorophyll fluorescence. *Plant Cell Physiol* 40: 1134–1142